

Shotgun approach based comparative proteomic analysis of *levor-tetrahydropalmatine*-induced apoptosis in hepatocytes

Chen Wang^{a,b,d,1}, Jiangrui Zhou^{c,1}, Shuowen Wang^{a,d}, Mingliang Ye^b, Guorong Fan^{a,d,*}, Hanfa Zou^b, Chunlei Jiang^{c,**}

^a Department of Pharmaceutical Analysis, School of Pharmacy, Second Military Medical University, No. 325 Guohe Road, Shanghai 200433, PR China

^b Division of Biotechnology, Dalian Institute of Chemical Physics, CAS, No. 457 Zhongshan Road, Dalian 116023, PR China

^c Laboratory of Stress Medicine, Department of Nautical Medicine, Second Military Medical University, No. 800 Xiangyin Road, Shanghai 200433, PR China

^d Shanghai Key Laboratory for Pharmaceutical Metabolite Research, No. 325 Guohe Road, Shanghai 200433, PR China

ARTICLE INFO

Article history:

Received 24 September 2009

Received in revised form 19 January 2010

Accepted 20 January 2010

Available online 28 January 2010

Keywords:

2D-nano-LC

Proteomics

Tetrahydropalmatine

Toxicity

ABSTRACT

The analgesic agent *levor-tetrahydropalmatine* (*l*-THP) was reported to be associated with acute or chronic hepatitis in clinical practice. We found that *l*-THP can induce apoptosis in the hepatocytes of BALB/c mice and human normal liver L-02 (L-02) cells. Several key molecules, including caspase-3, Bcl-2, BAD and Bax, were modulated by *l*-THP treatment. A novel high-throughput proteomic approach based on 2D-nano-LC-MS/MS was applied to simultaneously evaluate the alterations of global protein expression involved in the response of *l*-THP treatment in L-02 cells. A total of 156 deregulated proteins were identified, among which 12 proteins play regulatory or constitutive roles in the apoptosis pathways. Further analyses of two proteins (mTOR and MEK2) by Western Blots confirmed that these proteins were expressed at lower levels in *l*-THP-treated L-02 cells compared with those of control. The current study provided detailed evidence to support that *l*-THP is capable of inducing apoptosis in mammalian liver cells and improve the understanding of mechanisms of *l*-THP-induced hepatotoxicity.

Crown Copyright © 2010 Published by Elsevier Ireland Ltd. All rights reserved.

1. Introduction

Due to limitations in current knowledge regarding mechanisms of hepatic toxicity, drug-induced liver injury (DILI) is still a significant clinical problem, and the incidence of DILI seems to be increasing with an increase in the number of new drug available. DILI has emerged as the most frequent cause for after-marketing withdrawal of medications, despite a rigorous preclinical and clinical review process, and it also accounts for more than 50% of the cases of acute liver failure in the United States today (Bissell et al., 2001). DILI is commonly classified into intrinsic (dose-dependent and predictable) vs. idiosyncratic (non-dose-dependent and unpredictable) hepatotoxicity (Holt and Ju, 2006; Russmann et al., 2009; Takikawa, 2009). The former is often caused by the direct action of a drug, or more often a reactive metabolite of a drug, against hepatocytes while the latter develops in only a small proportion of subjects

(less than 1 per 10,000) expose to a drug in therapeutic doses, which can be further classified into allergic vs. non-allergic hepatotoxicity. More than 600 drugs have been associated with hepatotoxicity, however, most DILI are unpredictable (Park et al., 2005). Expansion of basic research into mechanisms of DILI is warranted.

Herbal medicines (HMs) have played important roles in clinical therapy in many oriental countries for thousands of years. Although the interest in their use among western populations is a relatively recent phenomenon, their frequency of use is growing explosively and is beginning to parallel and even exceed that of conventional medications (Seefl, 2009). However, HMs contain multiple ingredients, not all of which are identifiable. The knowledge on safety and efficacy is lacking because few HMs have been evaluated by rigorous scientifically designed trials. Herbal hepatotoxicity is increasingly recognized as the use of these medications has increased, and DILI from HMs seems to be a serious problem all over world now (Stickel, 2007; Takikawa, 2009). The recent evidence on hepatotoxic events associated with the use of herbal medicinal products has been reviewed (Pittler and Ernst, 2003).

Corydalis yanhusuo also called *Rhizoma corydalis* is well known as an analgesic agent in traditional Chinese medicines for thousands of years. Tetrahydropalmatin is one of the main active ingredients isolated from *Corydalis yanhusuo*. The stereoselective pharmacokinetic results showed that plasma C_{max} and $AUC_{0-\infty}$ ratios (l/d) of THP were 2.91 and 2.84, respectively, after administration of 5 mg/kg of

* Corresponding author at: School of Pharmacy, Second Military Medical University, 325 Guohe Road, Shanghai 200433, PR China. Tel.: +86 21 8187 1260; fax: +86 21 8187 1260.

** Corresponding author.

E-mail addresses: Guorongfan@yahoo.com.cn (G. Fan), cjiang@vip.163.com (C. Jiang).

¹ These two authors are contributed equally to this work.

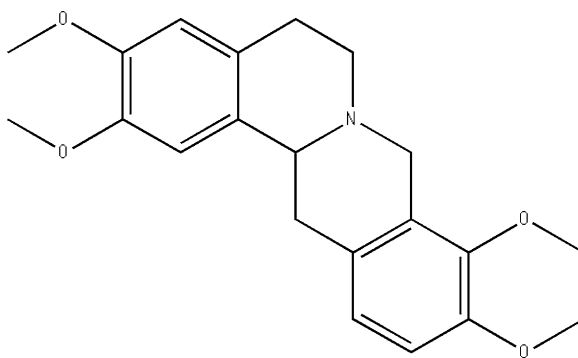


Fig. 1. Chemical structure of *L*-tetrahydropalmatine.

rac-THP in rats (Hong et al., 2008). *Levo*-tetrahydropalmatine (*L*-THP, Fig. 1), which is officially listed in the Chinese pharmacopoeia was demonstrated to have excellent analgesic effects and has been in use in clinical practice for years in China (Chu et al., 2008). However, the clinical practice of this analgesic drug has been associated with human poisonings (Lai and Chan, 1999). Several case reports associate the development of acute or chronic hepatitis with the chronic ingestion of “Jin Bu Huan Anodyne Tablets”, which contains purified, concentrated *L*-THP, and the clinical features of this illness included fever, fatigue, nausea, pruritus, abdominal pain, jaundice, and hepatomegaly (Barceloux, 2008). In a case series of 7 patients, the mean onset of acute hepatitis after beginning intake these tablets was 20 weeks (range: 7–52 weeks), and biopsy specimens showed that one patient had hepatitis with eosinophils and one patient had mild hepatitis, moderate fibrosis, and microvesicular steatosis (Woolf et al., 1994). A case of chronic liver damage was reported in a 49-year-old man 2 months after beginning Jin Bu Huan intake which including biopsy-proven chronic hepatitis with moderate fibrosis (Picciotto et al., 1998). Although the reported toxic effects of *L*-THP included depression of neurologic and cardiovascular function, the most reported toxic effects are acute or chronic hepatitis (Horowitz et al., 1996; Kaptchuk, 1995; Picciotto et al., 1998; Woolf et al., 1994).

In our study, we found severe hepatic injury subsequent to intake of *L*-THP in BALB/c mice. Further studies showed that *L*-THP can induce apoptosis in hepatocytes. Given the lack of information on mechanism of *L*-THP induced hepatocytes apoptosis, we employed a novel high-throughput proteomic approach based on online 2D-nano-LC-MS/MS to investigate the possible signaling pathways involved in the process. By comparative proteomic analysis of *L*-THP-treated L-02 cells and untreated control, we identified 156 differentially expressed proteins which are involved in energy generation, cytoskeleton, nucleic acid metabolism and apoptosis. Proteins associated with apoptosis were selected for further discussion and Western Blots was carried out to validate the differential expression pattern of the identified proteins. In company with the biochemical tests for apoptosis, we concluded that *L*-THP-induced apoptosis in hepatocytes might be a consequence of expression level changes of several important proteins which play regulatory or constitutive roles in apoptosis pathways.

2. Materials and methods

2.1. Materials

Levo-tetrahydropalmatine sulfate (optical purity $\geq 99.5\%$) was provided by Nanning Pharmaceuticals (Guangxi, China). Dithiothreitol (DTT), iodoacetamide (IAA), Triton X-100, PMSF and Tris were purchased from Sino-American Biotechnology Corporation (Beijing, China). Urea, ammonium acetate, trypsin, protease inhibitor cocktail (EDTA free) was purchased from Roche (Penzberg, Germany). Anti-MEK2, anti-mTOR, anti-Bax, anti-Bcl-2, anti-BAD and anti- β -actin antibodies were purchased from Cell Signal Technology (Danvers, MA, USA). Antibodies

against caspase-3 and anti-rabbit IgG labeled with HRP were purchased from Santa Cruz Biotechnology (Santa Cruz, CA, USA). HPLC-grade acetonitrile was obtained from Merck Company (Darmstadt, German). Double-distilled water was used for the preparation of all solutions.

2.2. Animals and cell cultures

Twelve 6-week-old male BALB/c mice were purchased from Shanghai SLAC Laboratory Animal Co. Ltd. (Shanghai, China). All animals received human care according to the criteria outlined in the Guide for the Care and Use of Laboratory Animals, which was prepared by the National Academy of Sciences and published by the National Institutes of Health. After 2 weeks of acclimatization, the mice were divided randomly into two groups ($n=6$ /group) as follows: *L*-THP group, intraperitoneal injection with *L*-THP at a single dose of 375 mg/kg; healthy control group, intraperitoneal injection with the same volume of 0.9% saline.

Human normal liver L-02 (L-02) cells were purchased from Shanghai Institute of Biochemistry and Cell biology, Chinese Academy of Science. The cells were cultivated in RPMI-1640 complete medium supplemented with 10% fetal bovine serum in a humidified atmosphere of 5% CO₂ at 37 °C. When cultivated to 80% confluence, L-02 cells were treated with 100 μ M *L*-THP or normal saline for 24 h.

2.3. Histopathology and immunohistochemistry

Mice were injected i.p. with 0.2 ml *L*-THP (amount to 375 mg/kg body weight) or normal saline 24 h before they were killed. Each liver was fixed in 10% formalin for 12 h and embedded in paraffin wax. Four-micrometer histologic sections of the paraffin-embedded tissues were stained with hematoxylin-eosin and then prepared for light microscopy. Terminal deoxynucleotidyl transfer as (TdT)-mediated dUTP nick-end-labeling (TUNEL) staining was performed on paraffin-embedded sections by using the *in situ* cell death detection kit (Roche, Penzberg, Germany). Immunostaining was performed by using primary antibodies mentioned above ($n=6$). The immunostaining area was quantified using image-pro 5.0.2 (Media Cybernetics, Silver Spring, MD, USA).

2.4. Cell viability

Cell viability was measured by the MTT (3-(4,5-dimethylthiazol-2-yl)-2,5-diphenyltetrazolium bromide) assay. Cells were seeded on 96-well tissue culture plates with 2×10^3 cells in 100 μ l media per well. After a 24 h stabilization of the cells, they were treated with 10, 50, 100 and 500 μ M concentrations of *L*-THP for 24 h, respectively. At the end of exposure, 40 μ l of MTT solution (5 mg/ml) was added and the cells were incubated for 4 h at 37 °C. Cells were solubilized with 150 μ M of DMSO and absorbance was quantified spectrophotometrically at 540 nm. The viability of the treated group was expressed as the percentage of control group which was assumed to be 100%.

2.5. Sample preparation for proteomic study

After treatment with 100 μ M *L*-THP or vehicles for 24 h, the L-02 cells were scraped using a cell scraper. For proteomic analysis, cells from three independent experiments were pooled in order to collate sufficient quantity of cells and at the same time to normalize biological variations. After washed two times with ice-cold of PBS, the cell pellet was suspended in 1 ml of extraction buffer (8 M urea, 50 mM Tris-HCl, pH 7.5, 0.25% (v/v) Triton X-100, 1 mM PMSF, 1 mM DTT, 1 \times protease inhibitor cocktail) and homogenized for 1 min. The homogenate was centrifuged at 20,000 rpm for 30 min at 4 °C, and the supernatant was mixed with five volumes of precipitation buffer (ethanol:acetone:glacial acetic acid 50:50:0.1). Precipitant was carried out at -20 °C overnight. After washed three times with cold acetone, the pellet was dissolved in denature buffer (8 M urea, 50 mM Tris-HCl, pH 8.3) in a concentration about 1 mg/ml. The samples was reduced by DTT at 37 °C for 2 h and alkylated by iodoacetamide in the dark at room temperature for 40 min. Then the solution was diluted to 1 M urea with 50 mM Tris-HCl (pH 8.3). Finally, trypsin was added at an enzyme-to-substrate of 1/25 (w/w) and incubated at 37 °C overnight. Then the digested mixture was desalting with a homemade C₁₈ solid-phase cartridge and stored at -80 °C before use.

2.6. 2D-nano-LC-MS/MS analysis and database searching

The 2D-nano-LC-MS/MS system consisted of a quaternary Surveyor pump and an LTQ linear IT mass spectrometer equipped with a nanospray source (Thermo, San Jose, CA, USA). The temperature of the ion transfer capillary was set at 200 °C. The spray voltage was set at 1.82 kV. All MS and MS/MS spectra were acquired in the data-dependent mode. The mass spectrometer was set that one full MS scan was followed by six MS/MS scans. The 2D-nano-LC/MS/MS analysis was carried out according to a reported method with minor modification (Wang et al., 2007). Briefly, the tryptic samples were dissolved in 0.1% (v/v) formic acid, loaded onto a monolith strong cation exchange (SCX) column (150 mm id \times 7 cm) automatically. Then a series stepwise elution with salt concentrations of 50, 100, 150, 200, 250, 300, 350, 400, 500, and 1 000 mM NH₄AC was used to gradually elute peptides from the phosphate monolithic column onto the C18 analytical column.

The MS/MS spectra were searched using SEQUEST (version 2.7) against a composite database including both original and reversed human protein database of International Protein Index (ipi.human 3.17.fasta, including 60 234 entries, <http://www.ebi.ac.uk/UniProt/UniProtHuman.html>). Cysteine residues were searched as a fixed modification of 57.0215 Da, and methionine residues were searched as a variable modification of 15.9949 Da. Peptides were searched using fully tryptic cleavage constraints and up to two missed cleavages sites were allowed for tryptic digestion. The mass tolerances are 2 Da for parent masses and 1 Da for fragment masses. Initial searching results were filtered with the following parameters as reported previously (Roth et al., 2006; Wan et al. 2006; Tian et al., 2008; Li et al. 2008): the $X_{corr} \geq 1.8$ for a singly charged peptide; 2.5 for a doubly charged peptide; and 3.5 for a triply charged peptides; the minimum ΔC_n cutoff value of 0.08.

For semiquantitative comparison of the proteins identified in *l*-THPs and the CONs, spectral counts for each identified protein from each experiment were extracted, averaged, normalized, and compared as described previously (Roth et al., 2006; Tian et al., 2008; Wan et al., 2007).

2.7. Protein validation by Western blots

After various treatments, proteins in the whole cell lysate were resolved on 10% SDS-PAGE and then transferred onto nitrocellulose membrane (Schleicher & Schuell,

Dassel, Germany). The membranes were blocked overnight in phosphate-buffered saline containing 10% nonfat dry milk and 0.5% Tween-20, and incubated with primary antibodies for 2 h. Horseradish peroxidase-conjugated anti-rabbit IgG was used as the secondary antibody. Target proteins were imaged with the ECL system (Pierce, Rockford, IL, USA). The bands were visualized and quantified using Quantity One imaging software (Bio-Rad). The intensities of Bax, Bcl-2, cleaved caspase 3 and BAD were adjusted by beta-actin intensity.

2.8. Statistics

Data are expressed as means \pm SD of n independent experiments. Statistical analysis were carried out by Student's *t*-test or by ANOVA followed by the Bonferroni test. $p < 0.05$ was considered significant.

3. Results

3.1. *l*-THP treatment induced apoptosis in the BALB/c mouse hepatocytes

Necrosis and apoptosis are two outcomes of drug-induced liver injury (Malhi et al., 2006). In order to evaluate the effects of *l*-THP

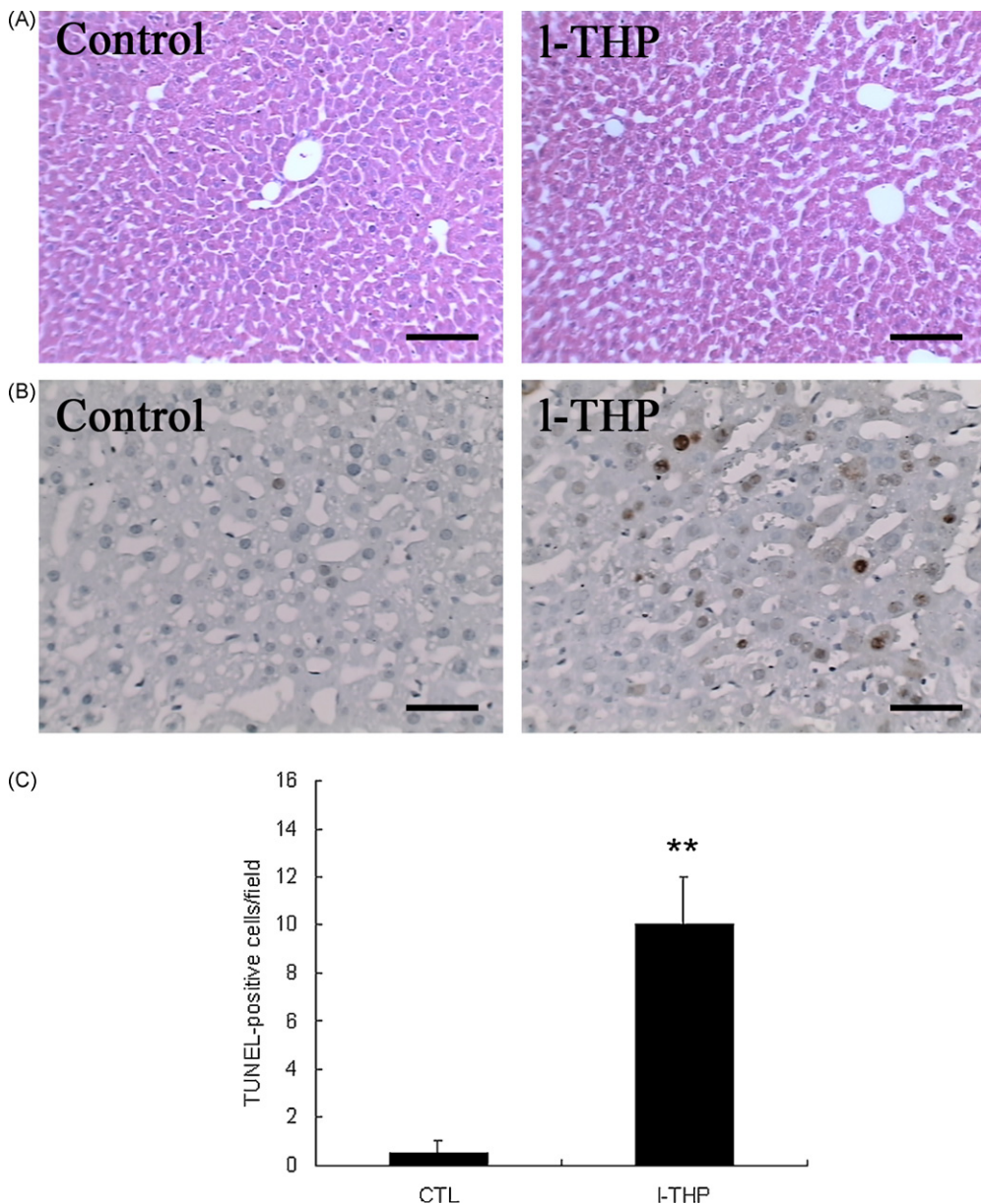


Fig. 2. (A) Detection of necrosis in the mouse liver by hematoxylin-eosin staining. *l*-THP-treated liver exhibited slight hepatocytes necrosis vs. the control group (scale bar, 100 μ m). (B) Detection of apoptotic hepatocytes in the liver slides by TUNEL staining 24 h after 375 mg/kg *l*-THP treatment. Brown staining indicates TUNEL-positive cells (scale bar, 50 μ m). Relative to the control group, the number of TUNEL-positive cells per field (110 ± 5 cells) was significantly increased. (C) Data represented the means \pm SD of six different experiments. **Significant difference compared with vehicle control ($p < 0.01$).

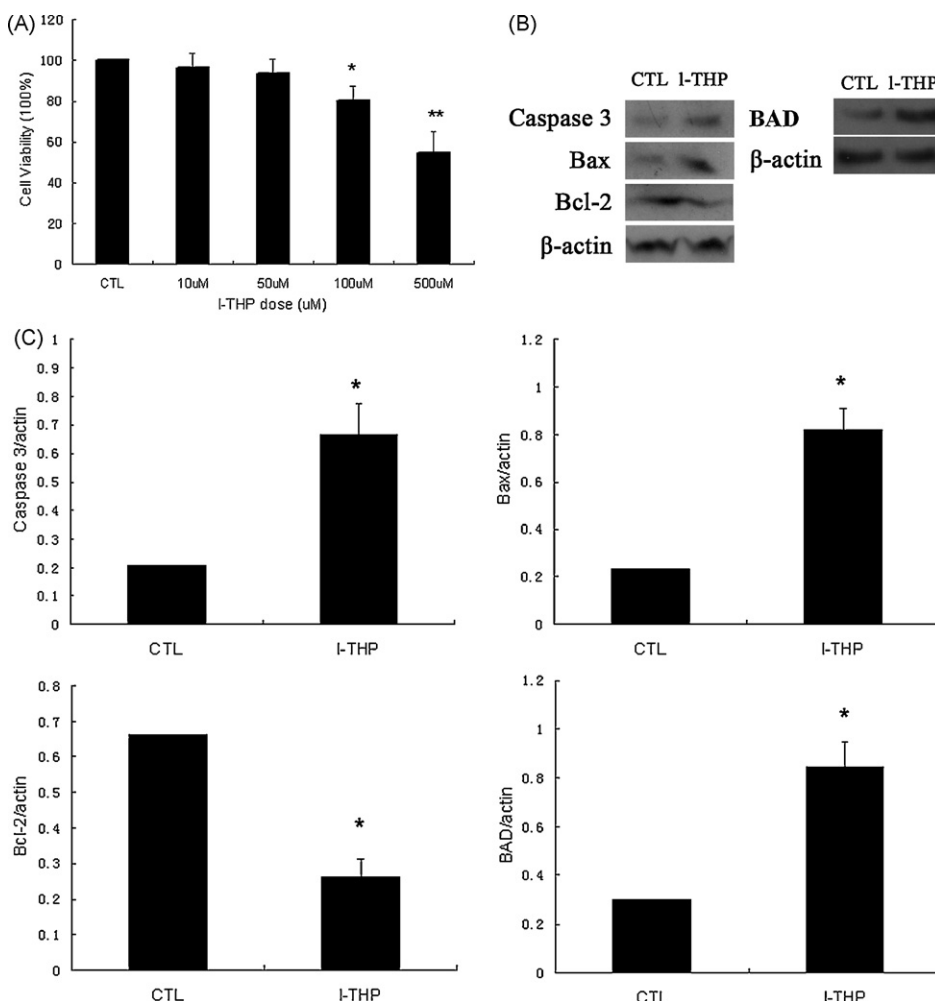


Fig. 3. (A) Effect of *I*-THP on L-02 cells death by MTT assay after 24 h treatment. Dose–response effect of *I*-THP on cell viability. Cells were plated at a density of 2×10^4 cells/ml in 100 μ l media per well and cultured at various concentrations (10, 50, 100 and 500 μ M). Cell viability was assayed using the 3-(4,5-dimethylthiazol-2-yl)-2,5-diphenyltetrazolium bromide (MTT) method. During the experiment, untreated cells served as controls. Values represented the means \pm SD of six different experiments and analyzed by the ANOVA followed by the Bonferroni test. *Significant difference compared with vehicle control ($p < 0.05$); **Significant difference compared with vehicle control ($p < 0.01$). B) Western blots analysis of apoptotic markers. Expression of apoptosis-related proteins (cleaved caspase-3, Bcl-2, BAD and Bax) in L-02 cells treated with 100 μ M *I*-THP or vehicle for 24 h. (C) Data shown are the results of three independent experiments and are represented as the relative densities of protein bands normalized to β -actin. Results are presented as means \pm SD of three assays. *Significant difference compared with vehicle control ($p < 0.05$).

treatment on hepatocyte, studies *in vivo* were carried out. Several dose levels (75, 150, 375 and 750 mg/kg which amount to 0.1, 0.2, 0.5 and 1 of IC50, respectively) (Jin, 2001) were tested. No significant necrosis/apoptosis were observed when the mice were treated at a single dose of 75 and 150 mg/kg. Histopathological assessment by hematoxylin-eosin staining showed no periacinar hepatocellular necrosis in mice ($n=6$) treated with 375 mg/kg *I*-THP after 24 h (Fig. 2A), however, significant differences in apoptosis was observed by the TUNEL assay (Fig. 2B). These observations together demonstrated that *I*-THP induced apoptosis in hepatocytes after 24 h treatment.

3.2. Expression of apoptosis-related proteins after *I*-THP treatment in L-02 cells

In order to avoid the possible individual variations in the response of the mouse liver to *I*-THP and improve the accuracy of the following cell signaling research, the stable cell line L-02, which has been used in the study of hepatotoxicity *in vitro* (Ji et al., 2002, 2005; Yao et al., 2008), was applied for the analysis of molecular mechanism underlying the *I*-THP-induced apoptosis. By means of MTT assay, the cytotoxicity profile of *I*-THP against L-02

cell lines was determined. Significant cytotoxicity was observed when the *I*-THP concentration reached to 100 μ M (Fig. 3A). Then, apoptotic markers such as Bax, Bcl-2, BAD and cleaved caspase-3 were detected by Western Blots to evaluate *I*-THP-induced apoptosis. Anti- β -actin antibody was used to normalize the optical density values. Immunoblots analyses were replicated three times. Fig. 3B and C summarizes the expression of proteins with proapoptotic or anti-apoptotic activity detected by Western blots analysis. Consistent with the proapoptotic effects of *I*-THP treatment, we found the

Table 1
Total spectral counts and proteins identified of CONs and *I*-THPs.

Sample	Total spectral counts	Total identified proteins
CON_1	42609	1987
CON_2	37441	1766
CON_3	38003	1773
<i>I</i> -THP_1	37948	1738
<i>I</i> -THP_2	35626	1645
<i>I</i> -THP_3	34178	1585

All data meet the following criteria: the $X_{corr} \geq 1.8$ for a singly charged peptide; 2.5 for a doubly charged peptide; and 3.5 for a triply charged peptides; the minimum ΔC_n cutoff value of 0.08.

Table 2List of the identified differentially expressed protein associate with apoptosis^a.

IPI	Protein name	Spectral counts ^b		
		CON	<i>l</i> -THP	Ratio ^c
IPI00026994	PRA1 family protein 2 (PRAF2)	0.2	3.82	19.11
IPI00021786	RAF proto-oncogene serine/threonine-protein kinase (Raf-1)	0.78	6.54	8.36
IPI00008868	Microtubule-associated protein 1B (MAP-1B)	0.89	5.68	6.37
IPI00307155	Rho-associated protein kinase 2	37.77	6.51	0.17
IPI00429689	Serine/threonine-protein phosphatase 2A catalytic subunit beta isoform	6.57	0.94	0.14
IPI00020567	Rho GTPase-activating protein 1	8.34	0.88	0.11
IPI00000041	Rho-related GTP-binding protein RhoB	8.46	0.88	0.10
IPI00296259	Transmembrane emp24 domain-containing protein 4	3.24	0.2	0.06
IPI00514068	Ras GTPase-activating-like protein IQGAP3	3.32	0.2	0.06
IPI00640341	FK506-binding protein 8	3.45	0.2	0.06
IPI00031410	FKBP12-rapamycin complex-associated protein (mTOR)	4.32	0.2	0.05
IPI00003783	Dual-specificity mitogen-activated protein kinase 2	6.19	0.2	0.03

^a The complete dataset of identified proteins with *l*-THP/CON (spectral count ratio) more than 5 or less than 0.2 is available in Table S1 of Supporting information.^b The raw spectral counts from each experiments were normalized (raw spectral counts for each identified protein were divided by the total spectral count number then multiplied by 100,000). Then the normalized values from the three *l*-THPs and CONs were averaged.^c Ratio of normalized, averaged *l*-THP to CON spectral counts. The spectral counts of zero were changed to 0.2 to avoid division by zero.

deregulation of Bcl-2 (down-regulated), Bax (up-regulated), BAD (up-regulated) and 17 kDa cleaved caspase-3 (up-regulated) were consistent with the proapoptotic effects of *l*-THP treatment.

3.3. 2D-nano-LC-MS/MS analysis and Western blots

A comprehensive shotgun proteomic profiling procedure, based on online 2D-nano-LC-MS/MS system was applied to uncover proteomic alterations associated with *l*-THP induced apoptosis. To maximize overall proteomic coverage and to control for the somewhat stochastic random under-sampling nature of tandem mass spectrometry, each protein extract was analyzed in triplicate using a linear ion trap instrument (Liu et al., 2004; Sandhu et al., 2005). The numbers of total spectral counts and identified proteins were listed in Table 1.

To improve the reliability of identification of the proteins, proteins meet the stringent filter criteria (the number of unique

peptide identified more than 2; protein identified at least two out of three runs) were included for the further semiquantitative analysis by spectral counts. Relative levels of protein expression were estimated based on the ratio of mean cumulative spectral counts detected for each protein in CONs and *l*-THPs. The spectral counts of both CONs and *l*-THPs were averaged, normalized, and compared. A total of 156 proteins with *l*-THP/CON (spectral count ratio) more than 5 (41 proteins) or less than 0.2 (115 proteins) were obtained as candidate proteins (Table S1). Functional information of the differentially expressed proteins was further explored on ExPasy (<http://www.expasy.org>) and by literature retrieval, and which play regulatory or constitutive roles in apoptosis pathways were listed in Table 2.

By doing literature survey of these proteins listed in Table 2, we found two molecules (mTOR and MEK2) can be closely involved in apoptosis process by affecting the expression of apoptosis-related proteins such as Bcl-2, Bax, BAD and caspases. Further validation of

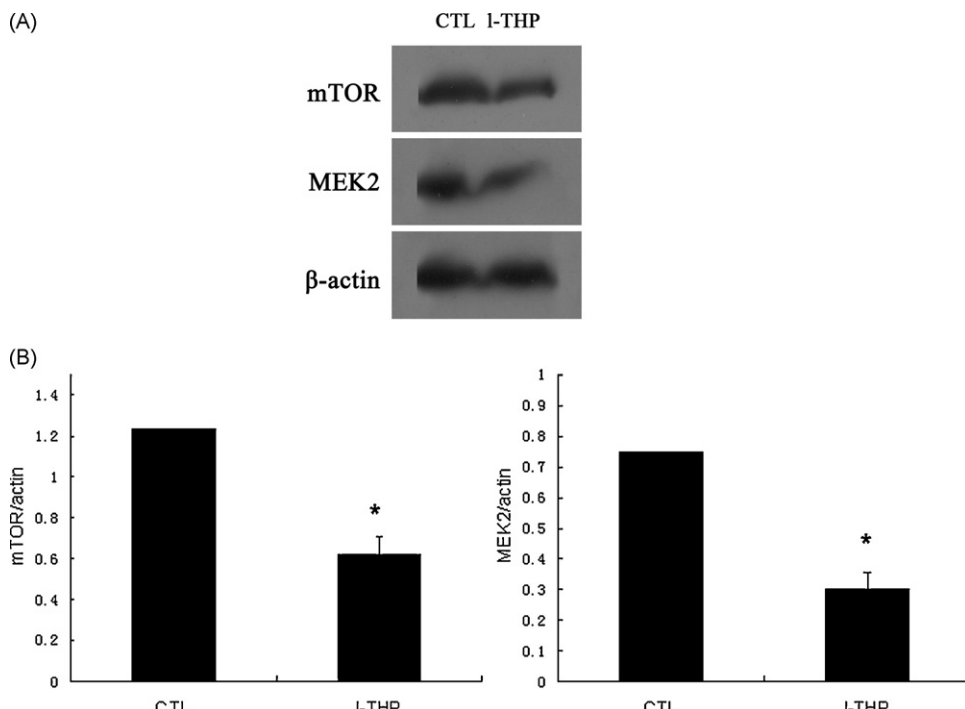


Fig. 4. (A) Modulation of mTOR and MEK2 by *l*-THP treatment of L-02 cells. L-02 cells were treated with 100 μM *l*-THP or vehicle for 24 h. (B) Data shown are the results of three different experiments and are represented as the relative densities of protein bands normalized to β-actin. Results are presented as means ± SD of three assays. *Significant difference compared with vehicle control ($p < 0.05$).

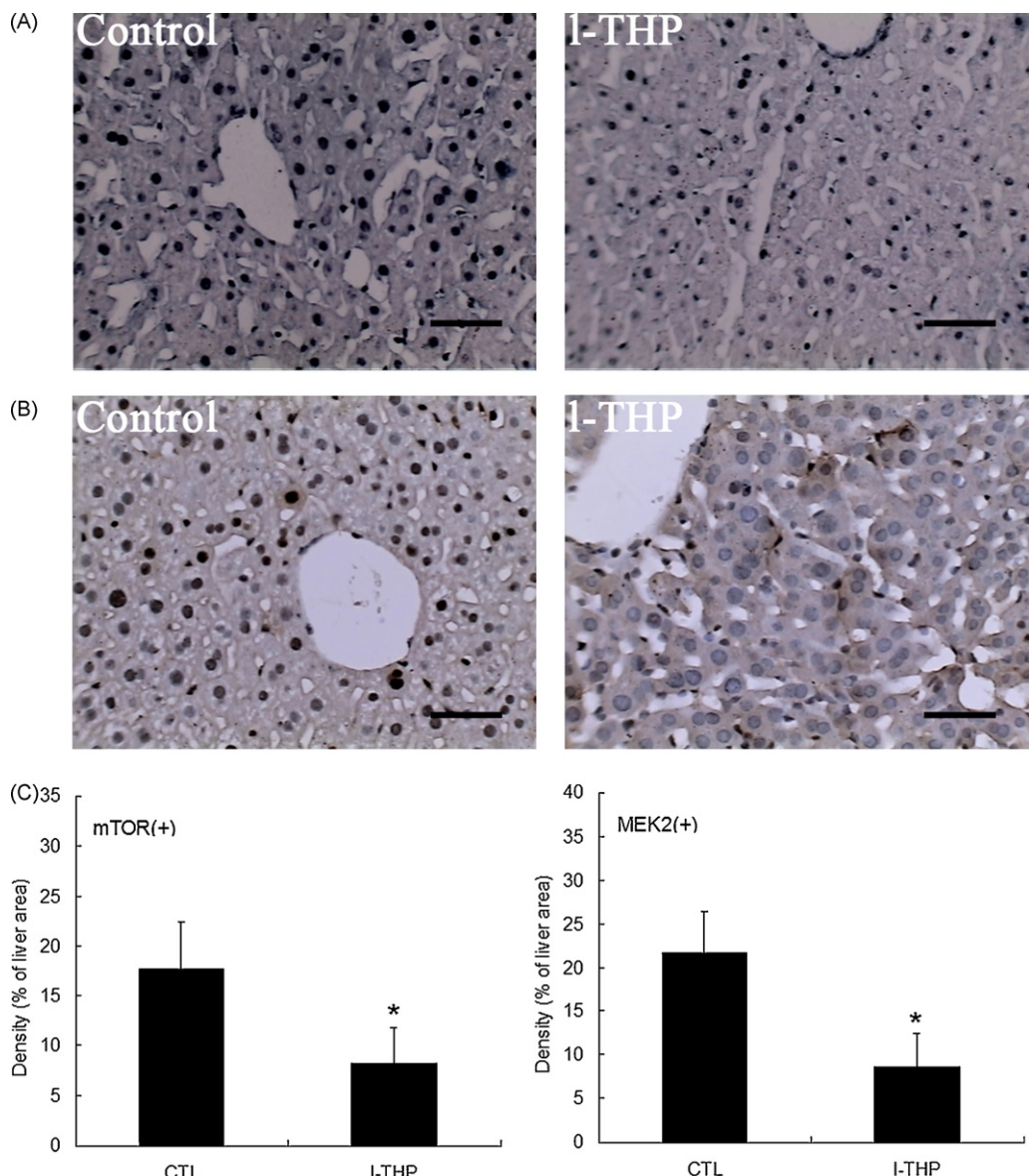


Fig. 5. Modulation of mTOR and MEK2 by *l*-THP treatment of mouse liver. (A) Detection of mTOR in the liver slides after 375 mg/kg *l*-THP treatment for 24 h. Blue staining indicates mTOR expression. (B) Detection of MEK2 in the liver slides after 375 mg/kg *l*-THP treatment for 24 h. Brown staining indicates MEK2 expression (scale bar, 50 μ m). The photos shown were representative of three independent experiments. C) The relative densities of target preprotein were measured by scanning of immunostaining area. Results are presented as means \pm SD of three assays. *Significant difference compared with vehicle control ($p < 0.05$).

these two proteins by Western Blots was carried out. Fig. 4 shows that the altered intensity of the proteins matched well with the differences obtained in 2D-nano-LC-MS/MS based proteomic analysis.

To determine whether *l*-THP induced the down-regulation of mTOR and MEK2 *in vivo*, immunohistochemical analyses were also performed in BALB/c mice. The two proteins, mTOR and MEK2, exhibited a similar expression pattern as the proteomic profile showed after *l*-THP treatment (Fig. 5).

4. Discussion

DILI is still unpredictable due to the limitations in the current knowledge of drug toxicity. Expansion of basic research into mechanisms of DILI is of great importance. However, over the past decade, researchers attempting to uncover the mechanisms of DILI, in the most case, focused on specific biochemical pathways. The advent of the global proteomic profiling based on shotgun

approach now allows the simultaneously evaluate the global proteins alterations which were resulted from the host response to the DILI. Therefore, this technology is a valuable tool for elucidating the mechanisms of DILI. In our study, this global proteomic method was applied to study the mechanisms of *l*-THP induced liver injury.

l-THP has received much attention as an analgesic agent in clinical practice. However, the clinical practice of this analgesic drug has been associated with human poisonings (Lai and Chan, 1999), and the most reported toxic effects are acute or chronic hepatitis (Horowitz et al., 1996; Kapchuk, 1995; Picciotto et al., 1998; Woolf et al., 1994). Therefore, it will be very important to uncover the molecular mechanisms of *l*-THP-induced liver injury. We found that *l*-THP treatments on mice lead to hepatocytes apoptosis. Similar results were obtained in L-02 liver cells. Cleavage of caspase-3, which are characteristics of apoptosis, were observed in *l*-THP-treated L-02 cells. Bcl-2 and Bax has been considered important regulators of apoptosis. Increase in the level of Bax and decrease in

the level of Bcl-2 were observed in the L-02 cells treated with *l*-THP after 24 h. These results suggested that intrinsic apoptosis pathway was involved the *l*-THP-induced hepatotoxicity.

Global proteome profiling was carried out to investigate *l*-THP induced cytotoxicity and apoptosis in the human liver cell line L-02. We have characterized the protein expression profile of L-02 cells after the *l*-THP treatment. A total of 156 deregulated proteins were obtained as candidate proteins. Through the functional analysis, we observed that the identified proteins are participating in different cell biological processes. Because of the limited sensitivity of mass spectrometry and low abundance of some signal proteins, most of the identified proteins are mainly engaged in the cellular organization and biogenesis or metabolism. Interestingly, a few proteins associated with apoptosis were identified and the proteins which function as key signaling integrators for apoptosis were summarized in Table 2. Here, we discussed some interesting proteins and their apoptosis-associated function in *l*-THP-induced DILI.

The FKBP12-rapamycin complex-associated protein, also known as mammalian target of rapamycin (mTOR), acts as a master switch of cellular catabolism and anabolism. Recently, mTOR has been found to play an important role in apoptosis (Castedo et al., 2002; Majumder et al., 2004; Pene et al., 2002). One of its downstream targets is ribosomal S6 kinase, which can bind to mitochondrial membranes and phosphorylate the proapoptotic molecule BAD on serine 136. This action can disrupt BAD's binding to Bcl-XL and Bcl-2 and thus inactivate BAD. In our study, we found that mTOR was down-regulated significantly in L-02 cells treated with *l*-THP after 24 h by proteomic assay and Western Blots. The altered mTOR expression might affect the normal function of BAD and thus influence Bcl-2 expression. Interestingly, we also observed increased level of BAD and decreased level of Bcl-2 in L-02 cells treated with *l*-THP. These results indicated mTOR, which act as one of the upstream regulator of BAD and Bcl-2, might be an important molecule involved in *l*-THP's proapoptotic effects. It was reported that PI3-K has a major role in the control of proliferation and apoptosis (Aoki et al., 2001; Raught et al., 2001). mTOR could be phosphorylated directly by Akt/PKB, so it would be possible that the proapoptotic effect is specific for the PI3K-Akt pathway. Further work needs to be done to elucidate the exact mechanisms.

MEK is a dual-specificity kinase that activates the extracellular signal-regulated kinase (ERK). It is the downstream of Ras/Raf pathway. The Raf/MEK/ERK signaling is one of the most well known signal transduction pathways because of its implication in a wide variety of cellular functions like cell proliferation, cell-cycle arrest, terminal differentiation and apoptosis (Belanger et al., 2003; MacCorkle and Tan, 2005; McCubrey et al., 2007; Liu et al., 2009). This pathway has profound effects on the regulation of the activity of many important proteins involved in apoptosis including Bad, Bim, Mcl-1, caspase-9 and Bcl-2 (McCubrey et al., 2007). Recent study showed that complete inhibition of MEK1/2 activity with PD184352 resulted in G1 arrest and induction of apoptosis (Squires et al., 2002). Our present study found that Bcl-2, which was considered as an important apoptosis regulator, was down-regulated after L-02 cells treated with *l*-THP. MEK2 expression level was also found down-regulated to a large extent by proteomic assay and Western Blots. Similar results were obtained *in vivo* by using immunohistochemical analysis. Interestingly, our proteomic data indicated that Raf proto-oncogene serine/threonine-protein kinase (Raf-1), which is direct upstream of MEK, was found up-regulated in *l*-THP group versus Control group. Raf-1 and MEK2 both play anti-apoptotic roles in process of apoptosis (Chen et al., 2001; Lau et al., 1998; von Gise et al., 2001). The deregulation of Raf-1 and MEK2 indicates *l*-THP might cause apoptosis in hepatocytes by influencing the Ras/Raf/MEK/ERK pathway. Although detailed analysis is required for further elucidation, we proposed that the significant reduction of MEK2 expression and deregulated Raf-1 would affect the nor-

mal function of the Ras/Raf/MEK/ERK pathway and thus induced apoptosis in *l*-THP-treated hepatocytes.

In addition to mTOR, MEK2, the expression levels of some other interesting molecules associated with apoptotic pathway were also influenced by *l*-THP treatment. The expression of rho-related GTP-binding protein RhoB precursor (RhoB) (Kong and Rabkin, 2005; Papadopoulou et al., 2008), PRA1 family protein 2 (PPAF2) (Li et al., 2001), microtubule-associated protein 1B (MAP1B) (Fifre et al., 2006; Lee et al., 2008) and serine/threonine-protein phosphatase 2A catalytic subunit beta isoform (PP2A) (Garcia et al., 2003) were altered during *l*-THP treatment. The precise roles of these identified molecules in *l*-THP-treated hepatocytes and the exact mechanisms of apoptosis-associated protein expression changes caused by *l*-THP need further study.

5. Conclusion

In conclusion, these results showed that comparative proteomics based on shotgun approach is a valuable tool for toxicity studies, since it allows the simultaneously evaluate the global proteins alterations which were resulted from the host response to the DILI. Deregulated proteins after *l*-THP treatment in L-02 liver cells were globally identified. Based on biochemical tests for apoptosis and proteomic survey, we concluded that *l*-THP-induced hepatocytes apoptosis might be a consequence of expression level changes of several important proteins which play regulatory or constitutive roles in apoptosis pathways. The current study improves the understanding of mechanisms of *l*-THP-induced liver injury, and provides prospects for the application of proteomics based on shotgun approach in the study of the mechanisms of DILI.

Conflict of interest

The authors declare that there are no conflicts of interest.

Appendix A. Supplementary data

Supplementary data associated with this article can be found, in the online version, at doi:10.1016/j.toxlet.2010.01.014.

References

- Aoki, M., Blazek, E., Vogt, P.K., 2001. A role of the kinase mTOR in cellular transformation induced by the oncoproteins P3k and Akt. Proc. Natl. Acad. Sci. U.S.A. 98, 136–141.
- Barceloux, D.G., 2008. Jin Bu Huan and tetrahydropalmatine. Med. Toxicol. Nat. Subst. Chapter 74, 518–521.
- Belanger, L.F., Roy, S., Tremblay, M., Brott, B., Steff, A.M., Mourad, W., Hugo, P., Erikson, R., Charron, J., 2003. Mek2 is dispensable for mouse growth and development. Mol. Cell. Biol. 23, 4778–4787.
- Bissell, D.M., Gores, G.J., Laskin, D.L., Hoofnagle, J.H., 2001. Drug-induced liver injury: mechanisms and test systems. Hepatology 33, 1009–1013.
- Castedo, M., Ferri, K.F., Kroemer, G., 2002. Mammalian target of rapamycin (mTOR): pro- and anti-apoptotic. Cell Death Differ. 9, 99–100.
- Chen, J., Fuji, K., Zhang, L.X., Roberts, T., Fu, H., 2001. Raf-1 promotes cell survival by antagonizing apoptosis signal-regulating kinase 1 through a MEK-ERK independent mechanism. Proc. Natl. Acad. Sci. U.S.A. 98, 7783–7788.
- Chu, H.Y., Jin, G.Z., Friedman, E., Zhen, X.C., 2008. Recent development in studies of tetrahydropyridoborberines: mechanism in antinociception and drug addiction. Cell. Mol. Neurobiol. 28, 491–499.
- Fifre, A., Sponne, I., Koziel, V., Kriem, B., Potin, F.T.Y., Bihain, B.E., Olivier, J.L., Oster, T., Pillot, T., 2006. Microtubule-associated protein MAP1A, MAP1B, and MAP2 proteolysis during soluble amyloid beta-peptide-induced neuronal apoptosis—synergistic involvement of calpain and caspase-3. J. Biol. Chem. 281, 229–240.
- Garcia, A., Cayla, X., Guergnon, J., Dessauge, F., Hospital, V., Rebollo, M.P., Fleischer, A., Rebollo, A., 2003. Serine/threonine protein phosphatases PP1 and PP2A are key players in apoptosis. Biochimie 85, 721–726.
- Holt, M.P., Ju, C., 2006. Mechanisms of drug-induced liver injury. Aaps J. 8, E48–E54.
- Hong, Z.Y., Le, R., Lin, M., Fan, G.R., Chai, Y.F., Yin, X.P., Wu, Y.T., 2008. Comparative studies on pharmacokinetic fates of tetrahydropalmatine enantiomers in different chemical environments in rats. Chirality 20, 119–124.

Horowitz, R.S., Feldhaus, K., Dart, R.C., Stermitz, F.R., Beck, J.J., 1996. The clinical spectrum of Jin Bu Huan toxicity. *Arch. Intern. Med.* 156, 899–903.

Ji, L.L., Zhao, X.G., Chen, L., Zhang, M., Wang, Z.T., 2002. Pyrrolizidine alkaloid clivorine inhibits human normal liver L-02 cells growth and activates p38 mitogen-activated protein kinase in L-02 cells. *Toxicol.* 40, 1685–1690.

Ji, L.L., Zhang, M., Sheng, Y.C., Wang, Z.T., 2005. Pyrrolizidine alkaloid clivorine induces apoptosis in human normal liver L-02 cells and reduces the expression of p53 protein. *Toxicol. In Vitro* 19, 41–46.

Jin, G., 2001. Discoveries in the Voyage of Corydalis Research. Shanghai Scientific & Technical Publishers, Shanghai, China, p. 50.

Kaptchuk, T.J., 1995. Acute hepatitis associated with Jin Bu Huan. *Ann. Intern. Med.* 122, 1636–1636.

Kong, J.Y., Rabkin, S.W., 2005. The association between RhoB and caspase-2: changes with lovastatin-induced apoptosis. *Biochem. Cell Biol.* 83, 608–619.

Lai, C.K., Chan, A.Y.W., 1999. Tetrahydropalmatine poisoning: diagnoses of nine adult overdoses based on toxicology screens by HPLC with diode-array detection and gas chromatography mass spectrometry. *Clin. Chem.* 45, 229–236.

Lau, Q.C., Brusselbach, S., Müller, R., 1998. Abrogation of c-Raf expression induces apoptosis in tumor cells. *Oncogene* 16, 1899–1902.

Lee, S.Y., Kim, J.W., Jeong, M.H., An, J.H., Jang, S.M., Song, K.H., Choi, K.H., 2008. Microtubule-associated protein 1B Light chain (MAP1B-LC1) negatively regulates the activity of tumor suppressor p53 in neuroblastoma cells. *FEBS Lett.* 582, 2826–2832.

Li, L.Y., Shih, H.M., Liu, M.Y., Chen, J.Y., 2001. The cellular protein PRA1 modulates the anti-apoptotic activity of Epstein-Barr virus BHRF1, a homologue of Bcl-2, through direct interaction. *J. Biol. Chem.* 276, 27354–27362.

Liu, H., Sadygov, R.G., Yates 3rd, J.R., 2004. A model for random sampling and estimation of relative protein abundance in shotgun proteomics. *Anal. Chem.* 76, 4193–4201.

Liu, J., Yang, Z., Li, A., Dong, J., 2009. Simultaneous inhibition of MEK and CDK4 leads to potent apoptosis in human melanoma cells. *Cancer Invest.* Epub ahead of print.

MacCorkle, R.A., Tan, T.H., 2005. Mitogen-activated protein kinases in cell-cycle control. *Cell Biochem. Biophys.* 43, 451–461.

Majumder, P.K., Febbo, P.G., Bikoff, R., Berger, R., Xue, Q., McMahon, L.M., Manola, J., Brugarolas, J., McDonnell, T.J., Golub, T.R., Loda, M., Lane, H.A., Sellers, W.R., 2004. mTOR inhibition reverses Akt-dependent prostate intraepithelial neoplasia through regulation of apoptotic and HIF-1-dependent pathways. *Nat. Med.* 10, 594–601.

Malhi, H., Gores, G.J., Lemasters, J.J., 2006. Apoptosis and necrosis in the liver: a tale of two deaths? *Hepatology* 43, S31–S44.

McCubrey, J.A., Steelman, L.S., Chappell, W.H., Abrams, S.L., Wong, E.W.T., Chang, F., Lehmann, B., Terrian, D.M., Milella, M., Tafuri, A., Stivala, F., Libra, M., Basecke, J., Evangelisti, C., Martelli, A.M., Franklin, R.A., 2007. Roles of the Raf/MEK/ERK pathway in cell growth, malignant transformation and drug resistance. *Biochim. Biophys. Acta* 1773, 1263–1284.

Papadopoulou, N., Charalampopoulos, I., Alevizopoulos, K., Gravanis, A., Stournaras, C., 2008. Rho/ROCK/actin signaling regulates membrane androgen receptor induced apoptosis in prostate cancer cells. *Exp. Cell Res.* 314, 3162–3174.

Park, B.K., Kitteringham, N.R., Maggs, J.L., Pirmohamed, M., Williams, D.P., 2005. The role of metabolic activation in drug-induced hepatotoxicity. *Annu. Rev. Pharmacol. Toxicol.* 45, 177–202.

Pene, F., Claessens, Y.E., Muller, O., Viguerie, F., Mayeux, P., Dreyfus, F., Lacombe, C., Bouscary, D., 2002. Role of the phosphatidylinositol 3-kinase/Akt and mTOR/P70S6-kinase pathways in the proliferation and apoptosis in multiple myeloma. *Oncogene* 21, 6587–6597.

Picciotto, A., Campo, N., Brizzolara, R., Giusto, R., Guido, G., Sinelli, N., Lapertosa, G., Celle, G., 1998. Chronic hepatitis induced by Jin Bu Huan. *J. Hepatol.* 28, 165–167.

Pittler, M.H., Ernst, E., 2003. Systematic review: hepatotoxic events associated with herbal medicinal products. *Aliment. Pharm. Therapeut.* 18, 451–471.

Raught, B., Gingras, A.C., Sonenberg, N., 2001. The target of rapamycin (TOR) proteins. *Proc. Natl. Acad. Sci. U.S.A.* 98, 7037–7044.

Roth, A.F., Wan, J.M., Bailey, A.O., Sun, B.M., Kuchar, J.A., Green, W.N., Phinney, B.S., Yates, J.R., Davis, N.G., 2006. Global analysis of protein palmitoylation in yeast. *Cell* 125, 1003–1013.

Russmann, S., Kullak-Ublick, G.A., Grattagliano, I., 2009. Current concepts of mechanisms in drug-induced hepatotoxicity. *Curr. Med. Chem.* 16, 3041–3053.

Sandhu, C., Connor, M., Kislinger, T., Slingerland, J., Emili, A., 2005. Global protein shotgun expression profiling of proliferating MCF-7 breast cancer cells. *J. Proteome Res.* 4, 674–689.

Seefl, L.B., 2009. Are herbs as safe as their advocates believe? *J. Hepatol.* 50, 13–16.

Stickel, F., 2007. Slimming at all costs: herbalife (R)-induced liver injury. *J. Hepatol.* 47, 444–446.

Squires, M.S., Nixon, P.M., Cook, S.J., 2002. Cell-cycle arrest by PD184352 requires inhibition of extracellular signal-regulated kinases (ERK) 1/2 but not ERK5/BMK1. *Biochem. J.* 366, 673–680.

Takikawa, H., 2009. Recent status of drug-induced liver injury. *Hepatol. Res.* 39, 1–6.

Tian, R.J., Li, L.D., Tang, W., Liu, H.W., Ye, M.L., Zhao, Z.B.K., Zou, H.F., 2008. Chemical proteomic study of isoprenoid chain interactome with a synthetic photoaffinity probe. *Proteomics* 8, 3094–3104.

von Gise, A., Lorenz, P., Wellbrock, C., Hemmings, B., Berberich-Siebelt, F., Rapp, U.R., Troppmair, J., 2001. Apoptosis suppression by Raf-1 and MEK1 requires MEK- and phosphatidylinositol 3-kinase-dependent signals. *Mol. Cell. Biol.* 21, 2324–2336.

Wan, J., Roth, A.F., Bailey, A.O., Davis, N.G., 2007. Palmitoylated proteins: purification and identification. *Nat. Protoc.* 2, 1573–1584.

Wang, F.J., Dong, J., Jiang, X.G., Ye, M.L., Zou, H.F., 2007. Capillary trap column with strong cation-exchange monolith for automated shotgun proteome analysis. *Anal. Chem.* 79, 6599–6606.

Woolf, G.M., Petrovic, L.M., Rojter, S.E., Wainwright, S., Villamil, F.G., Katkov, W.N., Michieletti, P., Wanless, I.R., Stermitz, F.R., Beck, J.J., Vierling, J.M., 1994. Acute hepatitis associated with the Chinese herbal product Jin Bu Huan. *Ann. Intern. Med.* 121, 729–735.

Yao, J.C., Jiang, Z.Z., Duan, W.G., Huang, J.F., Zhang, L.Y., Hu, L., He, L., Li, F., Xiao, Y.J., Shu, B., Liu, C.H., 2008. Involvement of mitochondrial pathway in triptolide-induced cytotoxicity in human normal liver L-02 cells. *Biol. Pharm. Bull.* 31, 592–597.